Int. J. Dev. Biol. 53: 139-147 (2009)
doi: 10.1387/ijdb.082745de

THE INTERNATIONAL JOURNAL OF DEVELOPMENTAL BIOLOGY
www.intjdevbiol.com

Generation of a reporter-null allele of *Ppap2b/Lpp3* and its expression during embryogenesis

DIANA ESCALANTE-ALCALDE*,[1,2], SARA L. MORALES[1] and COLIN L. STEWART[2,#]

[1]*Departamento de Neurociencias, Instituto de Fisiología Celular, Universidad Nacional Autónoma de México and* [2]*Cancer and Developmental Biology Laboratory, NCI-Frederick, Maryland, USA*

ABSTRACT Our knowledge of how bioactive lipids participate during development has been limited principally due to the difficulties of working with lipids. The availability of some of these lipids is regulated by the Lipid phosphate phosphatases (LPPs). The targeted inactivation of *Ppap2b,* which codes for the isoenzyme Lpp3, has profound developmental defects. Lpp3 deficient embryos die around E9.5 due to extraembryonic vascular defects, making difficult to analyze its participation in later stages of mouse development. To gain some predictive information regarding the possible participation of Lpp3 in later stages of development, we generated a *Ppap2b* null reporter allele and it was used to establish its expression pattern in E8.5-13.5 embryos. We found that *Ppap2b* expression during these stages was highly dynamic with significant expression in structures where multiple inductive interactions occur such as the limb buds, mammary gland primordia, heart cushions and valves among others. These observations suggest that Lpp3 expression may play a key role in modulating/integrating multiple signaling pathways during development.

KEY WORDS: *Ppap2b, Lpp3, reporter allele, expression*

Introduction

Participation of bioactive lipid-mediated signaling in the regulation of a wide variety of cellular processes has gained extensive attention during the past two decades. However our knowledge on the contribution of lipid-mediated signals to developmental processes has progressed slowly. Most of the information regarding bioactive lipid participation during development has arisen from studies involving the use of inactivating mutations of their receptors and/or their synthesizing or metabolizing enzymes (Brindley, 2004, Mizugishi *et al.*, 2005, Saba, 2004, Tanaka *et al.*, 2006, van Meeteren *et al.*, 2006).

Lipid phosphate phosphatases (LPPs) are a group of integral membrane enzymes that participate in intracellular lipid metabolism. Moreover, they regulate the biological activity and signaling of several bioactive phospholipids such as phosphatidic acid (PA), diacylglycerol (DAG), lysophosphatidic acid (LPA), sphingosine-1-phosphate (S1P), ceramide-1-phosphate (C1P) and ceramide (Brindley *et al.*, 2002, Brindley and Waggoner, 1998) controlling the availability of their phosphorylated substrates and dephosphorylated products. Subcellular localization of LPPs depends on the cell type and on physiological conditions (Jia *et al.*, 2003, Kai *et al.*, 2006, Sciorra and Morris, 1999, Sigal *et al.*, 2005, Sun *et al.*, 2004). Intracellular LPPs control the balance between PA and DAG therefore alter cell signaling mediated by these lipids and the synthesis of choline- and inositol- containing phospholipids. They play a fundamental role in the hydrolysis of phospholipase D (PLD)-derived PA and, in consequence, modulate PLD-mediated signaling. Some of the targets of PLD-derived PA are PI4PK, Sos, Raf and mTOR while RasGRP1 is regulated by LPP-derived DAG (McDermott *et al.*, 2004, Mor *et al.*, 2007, Zhao *et al.*, 2007). A role in the regulation of the intracellular pools of other lipids has been demonstrated for S1P (Long *et al.*, 2005) although involvement in the conversion of C1P to ceramide is also possible. LPPs localized in the plasma membrane serve to attenuate the receptor-mediated signaling of extracellular LPA and S1P, which

Abbreviations used in this paper: LPP, lipid phosphate phosphatase; PPAP, phosphatidic acid phosphatase.

***Address correspondence to:** Diana Escalante-Alcalde. Instituto de Fisiología Celular-UNAM, Circuito Exterior s/n Ciudad Univesitaria, México D. F. 04510, Coyoacán. Fax: +5255-5622-5607. e-mail: descalante@ifc.unam.mx web: http://www.ifc.unam.mx/faculty/descalan.html

[#] **Present address:** Institute of Medical Biology, Agency for Science, Technology and Research, Singapore

Accepted: 14 August 2008. *Published online:* 28 November 2008. *Edited by:* Edward De Robertis.

ISSN: Online 1696-3547, Print 0214-6282

in turn activate a wide variety of signaling pathways such as PLC/Ca^{++}, Ras/ERK/MAPK, Rac, Rho and PI3K (Brindley, 2004, Moolenaar *et al.*, 2004, Pyne *et al.*, 2004). Furthermore, biological actions independent of their catalytic activity have been proposed for some LPPs (Escalante-Alcalde *et al.*, 2003, Humtsoe *et al.*, 2003, Zhao *et al.*, 2005).

Most of the information regarding the participation of LPPs in specific cellular processes has stemmed from *in vitro* experiments. However, research performed during the last ten years has demonstrated their important contribution to development. In *Drosophila*, *wunen* and *wunen2* are required for proper germ cell migration and survival (Hanyu-Nakamura *et al.*, 2004, Renault *et al.*, 2004, Starz-Gaiano *et al.*, 2001, Zhang *et al.*, 1997). Furthermore, *wunen* also participates in proper neuron synaptogenesis and in the establishment of intestinal left-right laterality (Kraut *et al.*, 2001, Ligoxygakis *et al.*, 2001). Additionally *lazaro* is involved in the turnover of phosphatidylinositol during the process of phototransduction (Garcia-Murillas *et al.*, 2006). In the mouse, out of the three Lpps identified, *Ppap2c/Lpp2* null-gene inactivation and a gene trap of *Ppap2a/Lpp1* are viable and fertile without any apparent phenotype (Zhang *et al.*, 2000, Lynch, pers comm.). In contrast, *Ppap2b/Lpp3* targeted inactivation results in profound developmental defects indicating the essential participation of Lpp3 in mouse embryo development. Lpp3 deficient embryos die around E9.5 due to extraembryonic vascular defects. With lower penetrance, earlier lethality is due to anterior-posterior patterning alterations related to the antagonistic effect of Lpp3 on the Wnt/β-catenin signaling pathway by a still poorly understood mechanism (Escalante-Alcalde *et al.*, 2003).

The early embryonic lethality of Lpp3 deficiency makes difficult the analysis of its participation in later stages of mouse development. One way to gain some predictive information regarding the possible participation of Lpp3 in later stages of development is through the detailed analysis of its expression pattern. In this study we describe the generation of a *Ppap2b* null reporter allele, which was used to establish its expression pattern in E8.5-13.5 embryos. Remarkably, *Ppap2b* expression during these stages was highly dynamic with significant expression in structures where multiple inductive interactions occur such as the limb buds, mammary gland primordia, heart cushions and valves among others.

Results

Despite the wide range of available information in databases regarding mRNA expression using microarray analysis, little is known about the tissue-specific expression pattern of Lpp3 during development. Here we describe the generation of a reporter null allele of *Ppap2b* by inserting the bacterial β-galactosidase gene (*lacZ*) in exon 3 (Fig. 1) by homologous recombination in embryonic stem (ES) cells, which was designated *Ppap2b*^{tm2Stw}. For convenience, we will refer to this allele as *Ppap2b*^{lacZ}. Heterozygous *Ppap2b*^{lacZ} mice were viable and fertile. Mating of heterozygous *Ppap2b*^{lacZ} on either 129/SvJ x C57BL/6J or a pure 129Sv/J background yielded animals only of wild type and heterozygous genotype indicating that this allele is embryonic lethal (57% +/-; 42% +/+; n= 218). The phenotype of homozygous *Ppap2b*^{lacZ} embryos from heterozygous intercrosses, was essentially identical to our formerly described null alleles *Ppap2b*^{tm1Stw} and *Ppap2b*$^{tm3.1Stw}$ (Escalante-Alcalde *et al.*, 2003, Escalante-Alcalde *et al.*, 2007). This was characterized by a delay in development when compared to wild type or heterozygous littermates (12 to 24 hours), absence of chorioallantoic fusion at the 6 somite stage, allantois compaction (Fig. 1E-F), impaired remodeling of the primary capillary plexus of the yolk sac and gastrulation defects with low penetrance (not shown). Furthermore, in the best-developed mutant embryos, persistence of open neural tube was frequent (Fig. 1G). The use of an IRES sequence in the targeting design allowed us to detect the endogenous transcriptional activity of *Ppap2b*. Intensity of β-galactosidase staining recorded before embryo death, correlated with the genotype being more intense in homozygous than in heterozygous embryos. The expression of *Ppap2b* during early mouse development (E6.5-E8.5) using this allele has been shown previously (Escalante-Alcalde *et al.*, 2003). In this work we described, in detail, the expression pattern of *Ppap2b* in E8.5-E13.5 embryos to gain some predictive information regarding the participation of Lpp3 during these developmental stages. We used heterozygous embryos to reveal *Ppap2b* expression as reported by the activity of β-galactosidase (β-gal) and compare these patterns with those obtained by whole mount *in situ* hybridizations and in some stages by whole mount immunohistochemistry to test the fidelity

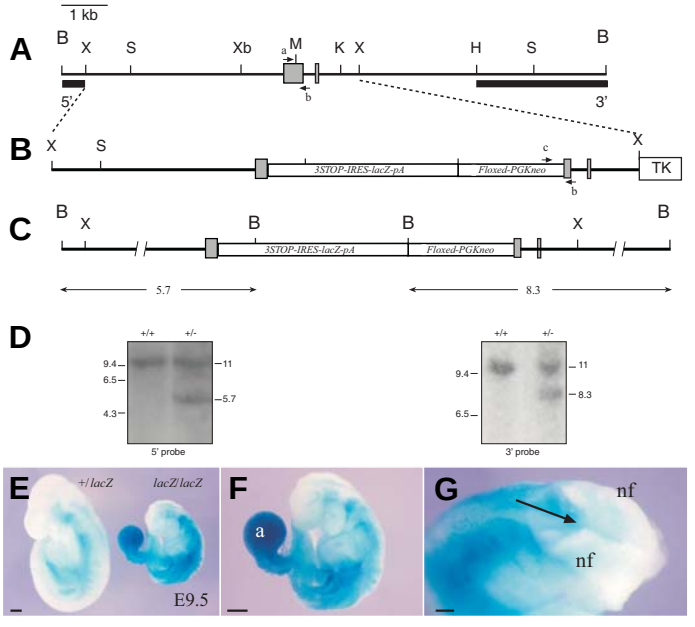

Fig. 1. Generation of the *Ppap2b*^{lacZ} allele. (A) *Genomic structure of the 11 kb BamHI fragment containing exons 3 and 4 of* Ppap2b *(gray boxes). Regions used as probes are indicated with black bars (5', 3'). Arrows with lower case letters show the position of oligonucleotides used for PCR genotyping.* **(B)** *Structure of the targeting construct. An IRES-lacZ-loxP-PGKneo-loxP cassette was introduced into the unique MunI site.* **(C)** *Structure of the targeted allele.* **(D)** *Southern blot of ES cells genomic DNA digested with BamHI and hybridized with the 5' and 3' probes.* **(E)** *E9.5* Ppap2b^{lacZ} *heterozygous and homozygous embryos.* **(F)** *Higher magnification of the mutant embryo in panel (E) showing allantois compaction and incomplete turning.* **(G)** *Dorsal view of the mutant embryo in panel (E) showing open neural tube at the midbrain and hindbrain (arrow). B, BamHI; H, HindIII; K, KpnI; M, MunI; S, SalI; X, XmaI; Xb, XbaI; a, allantois; nf, neural folds. Scale bar, 200 μm in (E,F); 100 μm in (G).*

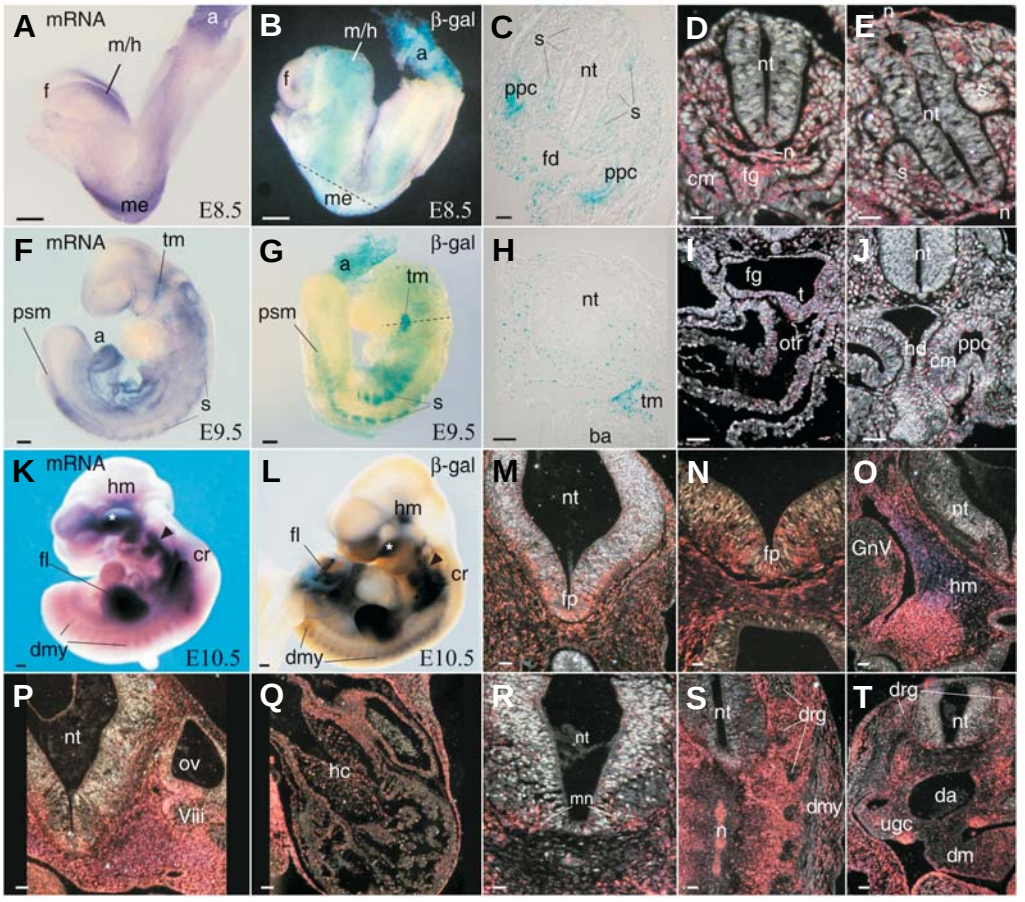

Fig. 2. *Ppap2b* expression in E8.5-10.5 embryos. *Whole mount* in situ *hybridization (mRNA) or β-galactosidase staining (β-gal) of* Ppap2b^{lacZ} *heterozygous mouse embryos at E8.5* **(A-E)**, *E9.5* **(F-J)** *and E10.5* **(K-T)**. **(C,H)** *Transverse sections at equivalent levels shown in (B,G) respectively (dashed lines) and photographed under Nomarski optics, β-gal staining appears in blue.* **(D-E, I-J, M-T)** *Transverse sections photographed under dark field illumination, β-gal staining appears pink or reddish. In some cases, strong β-gal staining is clearly observed in blue or purple color* **(N-P)**. *a, allantois; ba, 1st branchial arch; cm, coelomic mesothelium; cr, cervical region mesoderm; da, dorsal aorta; dm, dorsal mesentery; dmy, dermomyotome; drg, dorsal root ganglion; f, forebrain; fd. foregut diverticulum; fg, foregut epithelium; fl, forelimb; fp, floor plate; GnV, trigeminal ganglion; hc, heart cushions; hd, hepatic diverticulum; hm, head mesenchyme; me, mesoderm; m/h, midbrain/hindbrain region; mn, motor neurons; n, notochord; nt, neural tube; otr, outflow tract; ov, otic vesicle; ppc, pericardial-peritoneal canal; psm, presomitic mesoderm; s, somite; t, thyroid primordium; tm, future tympanic membrane; ugc, urogenital crest; Viii, acoustic neural crest cells. Asterisk and arrowhead in* **(K,L)** *show expression in the maxillary component of the first branchial arch and in the second branchial arch respectively. Scale bars, 100 μm in (A,B,F,G); 200 μm in (K,L); 20 μm in (C-E, N,R) and 40 μm in (H-J, M,O,P,Q,S,T).*

of the patterns obtained. As shown in Figures 2 and 4, mRNA, protein and β-gal expression patterns were essentially identical with few differences in β-gal intensity (likely due to its stability) and to the amount of Lpp3 protein in some neural structures (see below). As discussed in the following section, due to the great sensitivity of this reporter, we detected structures showing even low levels of *Ppap2b* expression. Cells expressing low-expression levels showed one (or a few) cytoplasmic granule while cells expressing higher levels of the enzyme showed a more homogeneous cytoplasmic staining.

Expression of Ppap2b *in E 8.5 mouse embryos*

In embryos Theiler stages (TS) 12-13, Lpp3 expression was abundant in the allantois and paraxial mesoderm but absent or weak in the forebrain and posterior embryonic domain respectively (Fig. 2A-B). Cells expressing β-gal were more abundant in the head and cervical mesoderm. The pericadial-peritoneal mesothelial cells and the somites showed conspicuous staining (Fig. 2C-E). β-gal activity was detected in cells along the gut endoderm being more intense at the level of the foregut diverticulum entrance (Fig. 2C-D). Expression was detectable in the neuroepithelium such as in the prospective midbrain, hindbrain and the ventral portion of the future spinal cord (Fig. 2 B-E). Furthermore, β-gal was expressed in the notochord (Fig. 2E) and in the region where it is organized at the level of the primitive streak. Reporter activity was found in the amnion and at lower activity in the visceral endoderm and vascular mesodermal cells of the yolk sac (not shown).

Expression of Ppap2b *in E9.5 mouse embryos*

In TS 14, regions exhibiting the strongest expression levels were the endoderm and ectoderm epithelia of the future tympanic membrane region followed by the allantois, somites, paraxial tissue at the cervical region and the developing intraembryonic coelomic cavity area (Fig. 2F-G). Sections through the embryos showed expression in the cephalic and cervical mesenchymal cells (Fig. 2H) with the exception of the mesenchyme in the telencephalic area. The otic vesicle epithelium and migratory neural crest tissue showed detectable expression (not shown). In the heart, cells in the wall of the outflow tract (Fig. 2I), the posterior wall of the common atrial chamber and few cells of the endocardial lining in the bulbo-ventricular canal showed reporter activity. Along the gut, expression was variable, with higher levels in the thyroid primordium, the ventral aspect of the foregut endoderm and lower levels present in the hepatic diverticulum, at the foregut-midgut junction and hindgut diverticulum (Fig. 2I-J). The strongest intraembryonic expression was in the mesothelial cells forming the pericardial-peritoneal coelomic cavity at the level of the developing forelimb (Fig. 2J). Expression in the notochord and developing nervous system followed the same expression pattern

as in the previous stage (Fig. 2H). In TS 15 embryos forelimb buds showed a strong β-gal staining in a group of scattered ectodermal cells in the ventral side of the developing forelimb (Fig. 3A).

Expression of Ppap2b*/Lpp3 in E10.5 mouse embryos*

In embryos TS 18, reporter activity was broadly found in the mesenchyme. In the cephalic and cervical regions, expression in the cephalic flexure mesenchyme and the one surrounding the primary head and anterior cardinal veins and dorsal aorta was more intense (Fig. 2K-L, N-P). Expression was also found in the mesenchyme of the anterior-distal aspect of the maxillary component of the first branchial arch and the second branchial arch (Fig. 2L). In the paraxial mesenchyme, expression was more abundant in the anterior (Fig. 2S) than in the posterior part (Fig. 2T) of the embryo correlating with de-epithelization of the somites into sclerotome cells. Expression in the dermomyotome of epithelialized somites was present in the caudal region whereas at the cervical and thoracic levels, expression was gradually restricted to the dorsal lip region of the dermomyotome (Fig. 2L). Expression in the notochord was more evident at this stage (Fig. 2S).

Staining in the heart area corresponded to the most dorsal aspect of the heart and the body wall overlaying the pericardial cavity. Detectable expression was found in the endocardial cushion tissue associated to the atrioventricular canal and in cells of the dorsal truncus arteriosus (Fig. 2Q). At this stage, expression in blood vessel endothelial cells was evident. The dorsal mesocardium as well as the mesenchyme surrounding the bronchus epithelium and oesophageal region of the foregut showed moderate β-gal activity (not shown). In the urogenital area, a bilateral stripe of mesothelial cells contiguous to the dorsal mesentery and the mesenchyme adjacent to the dorsal aorta showed reporter activity (Fig. 2T).

Expression was also detected in some components of the central and peripheral nervous systems at this stage. Forebrain neuroepithelium was devoid of significant reporter expression. Detectable expression in this and other regions of the neural tube correlated with invading blood vessels from the perineural vascular plexus. At the midbrain, hindbrain and cervical regions, cells expressing β-gal were found in the basal and floor plates (Fig. 2M-P) while a group of presumptive motor neurons showed reporter activity at the thoracic and lumbar areas (Fig. 2R). In the eye, detectable expression was found in the central domain of the outer layer of optic cup and lens pit (not shown). *Ppap2b* was also expressed in neural crest derivatives. In the trigeminal crest tissue, facio-acoustic (VII-VIII) neural crest complex and other developing cervical ganglia, expression was evident in certain groups of cells (Fig. 2O-P). Stronger expression levels were observed in the interacting region between the otic vesicle epithelia and the neural crest cells of the acoustic preganglion (Fig. 2P). The dorsal root ganglia showed a low but still detectable activity of β-gal. Unexpectedly, in contrast with the level of β-gal activity found in neural derivatives, Lpp3 immunohistochemistry showed a very strong staining in projecting axons of cranial ganglia and motor neurons. Furthermore, a weak expression in the ependyma of the spinal cord was evidenced (Fig. 4H).

In the limbs, the apical ectodermal ridge (AER) is the structure with strongest expression of *Ppap2b* at this stage. In the forelimbs moderate expression was found in the progress zone (PZ) region and the proximal dorsomedial mesenchyme, though expression in the PZ area was more restricted to the dorsal side (Figs. 3B-C, 4I).

Expression of Ppap2b*/Lpp3 in E11.5 mouse embryos*

Ppap2b expression pattern was essentially the same as that observed in E10.5. However, modification in the expression pattern of some structures was observed. Expression in the AER of limbs was preserved though weaker staining was observed in the superficial dorsomedial mesenchyme of the zeugopod. A region expressing strong reporter activity was present in the dorsal-central domain of the autopod and a weak expression indicated the future digital domains of the forelimb (Fig. 3D). Expression of β-gal in the developing mammary gland placodes 3 and 4 was evident at this stage (Fig. 3D). At the hindlimb level, the paraxial mesenchyme ventral to the inter dorsal root ganglia space expressed abundant reporter activity. Expression in the urogenital sinus area and umbilical hernia was stronger than in previous stages. Dermal expression in the cervical area became evident at this developmental stage.

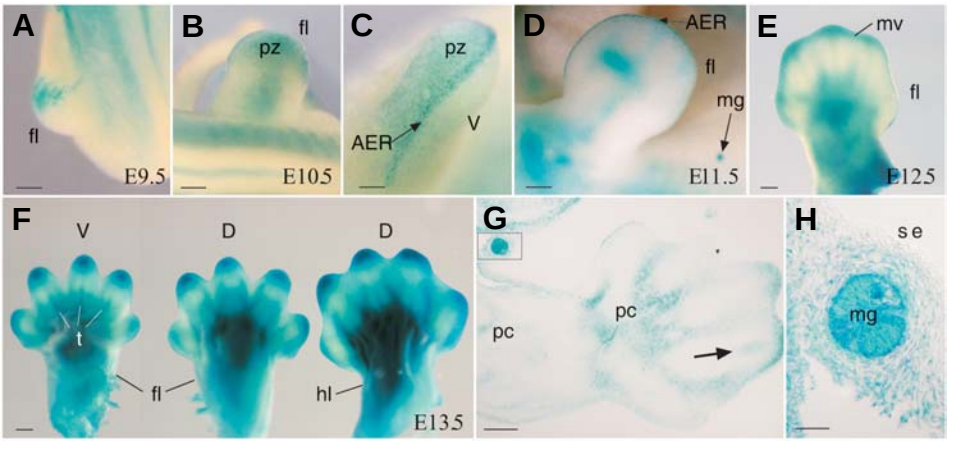

Fig. 3. *Ppap2b* expression during limb development. *β-galactosidase staining of limbs of E9.5* **(A)**, *E10.5* **(B,C)**, *E11.5* **(D)**, *E12.5* **(E)** *and E13.5* **(F,G)**. Ppap2b^{lacZ} *heterozygous embryos.* **(B,C)** *Dorsal and lateral views of a forelimb respectively.* **(G)** *Longitudinal section of a forelimb at E13.5; arrow shows expression in the central domain of the digit.* **(H)** *Higher magnification of the boxed area in (G) showing expression in the mammary gland epithelium. AER, apical ectodermal ridge; D, dorsal view of the limb; fl, forelimb; hl, hindlimb; mg, mammary gland; mv, mesenchyme surrounding the marginal vein; pc, perichondrium; pz, progress zone; se, surface ectoderm; t, tendon; V, ventral view of the limb. Scale bars, 100 μm in (A,C); 200 μm in (B, D-G) and 40 μm in (H).*

Expression of Ppap2b *in E12.5 mouse embryos*

In this stage, expression in the dermis had extended and the five pairs of mammary gland placodes showed abundant Lpp3 expression. The head mesenchyme showed abundant expression being more evident around the primary head vein and the cephalic ganglia. *Ppap2b/* Lpp3 expression was detected in the most ante-

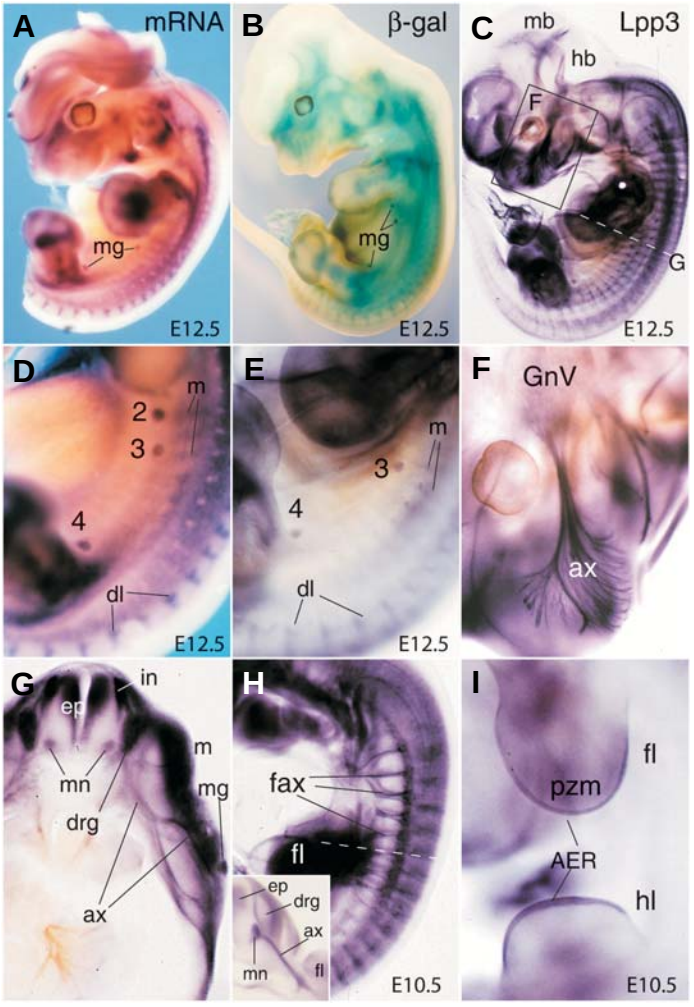

Fig. 4. *Ppap2b*-Lpp3 expression patterns in E10.5 and 12.5 embryos. *Whole mount* in situ *hybridization* **(A,D)**, *β-gal staining* **(B)** *and whole mount immunohistochemistry* **(C, E-I)** *in E12.5* **(A-G)** *and E10.5* **(H,I)** *embryos. In E12.5 embryos, differences in mRNA* **(A)**, *β-gal* **(B)** *and protein* **(C)** *expression patterns are mainly due to the great abundance of Lpp3 protein in growing axons. mg, mammary gland; mb, midbrain; hb, hindbrain.* **(D)** *Higher magnification of the interlimb area of the embryo in (A) showing* Ppap2b *mRNA expression in the mammary gland primordia (numbers).* **(E)** *Interlimb area of an E12.5 embryo showing Lpp3 protein expression in the mammary gland primordia (numbers).* **(F)** *Magnification of the boxed area in panel (C) showing a weak staining in the body of the trigeminal ganglion (GnV), but strong Lpp3 expression in projecting axons (ax).* **(G)** *Transverse section at the level indicated in panel (C) (dashed line) showing Lpp3 expression in a group of dorsal interneurons (in), the ependymal layer (ep), a subset of motor neurons (mn), dorsal root ganglion (drg) and projecting axon (ax). m, myotome; mg, mammary gland. In earlier embryos (E10.5), expression of Lpp3 protein in neural derivatives* **(H)** *such as the fasiculated axons (fax) projecting to the cervical or forelimb areas is also more evident by immunohistochemistry. Insert: transverse section at the level indicated by the white dashed line. In contrast, expression in non-neural tissue is essentially identical to the expression pattern obtained using the reporter allele. For instance, in the limb buds* **(I)**, *staining was found in the apical ectodermal ridge (AER) and progress zone mesenchyme (pzm) of the forelimb (fl). hl, hindlimb.*

rior myotomes at the inter limb area and more restricted to their dorsal lip in the rest of the embryo (Fig. A-B and D-E). Expression was found in the tail somites but absent in its distal extremity. The liver and heart did not show significant *Ppap2b* expression except for the atrioventricular endocardial cushions (not shown). In the genitourinary system, expression was found in the mesonephric ducts epithelium and urethral plate epithelium in addition to the deep mesenchyme of the genital tuberculum (not shown).

In the CNS, expression in the central domain of the optic cup was preserved however reporter activity in the optic stalk and developing hyaloid plexus was apparent at this stage (not shown). Expression domains in the ventral midbrain, hindbrain, spinal cord and peripheral structures were essentially as in the previous stage, but new expression domains became apparent by immunostaining, such as a group of spinal dorsal interneurons (Fig. 4C and G). Weak expression levels were also detected in the infundibulum neuroepithelium and the thalamus ventricular area. A graded expression of β-gal was observed in dorsal root ganglia being stronger in posterior than in anterior ganglia.

Expression in the AER was gradually down regulated between E11.5 and E12.5. While expression in the AER disappeared, expression in the mesenchyme surrounding the marginal vein was evident but stronger in the distal region of the prospective digits. The dorsal central domain of expression in the autopod was wider. Expression in the dorsal muscle anlagen was evident in the developing limbs (Fig. 3E, 4A-B).

Expression of Ppap2b *in E13.5 mouse embryos*

β-gal expression was widely distributed at this stage. However, reporter activity in the surface ectoderm, in most of the endoderm-derived epithelia, liver, heart muscle, condensed cartilage and the follicles of vibrissae, was very low or undetectable (Fig. 5). In the heart, the developing atrioventricular valves, atrium and vena cava showed reporter activity (Fig. 5 C-F). β-gal staining varied from strong to moderate in the perichondrium tissue and in some regions of highly differentiated cartilage (Fig. 5C, F-G). In the limbs, expression was found in the perichondrium of developing skeletal elements, the most central cells of the developing digits and the tip of the digits (Fig. 3F-G). Expression was also evident in the dorsal and ventral muscle anlagen (not shown) and developing ventral tendons (Fig. 3F). The mammary gland epithelia showed strong reporter activity while in the surrounding mesenchyme was weaker (Fig. 3G-H, 4A).

In the brain, β-gal expression was restricted to some structures such as the developing cerebral cortex and the ventricular area of the mesencephalon, rhombencephalon and cerebellum primordium (Fig. 5C and data not shown). In the spinal cord, a stripe of β-gal positive cells running along the central domain of the ependymal layer was observed and a weaker staining extended to the whole ependymal layer (Fig. 5H-I). Dorsal root ganglia showed a low but still detectable level of reporter activity (Fig. 5C, F and H).

Discussion

The mouse Lpp3 belongs to a group of enzymes with the potential to regulate/modulate a wide variety of signaling pathways. This would initially suggest a ubiquitous expression for this enzyme. Nonetheless, our previous (Escalante-Alcalde *et al.,* 2003) and present data show that, Lpp3 displays a very dynamic

and specific expression pattern during mouse embryo development.

Our analysis revealed that the reporter allele clearly reflected the endogenous mRNA expression pattern however the amount of Lpp3 protein did not correlate with the relative transcription levels found in central and peripheral nervous structures. For instance, in dorsal root ganglia or the motor neurons in the spinal cord, while the β-gal activity or amount of mRNA were very low, protein levels were much more robust. Furthermore, the protein content in developing nerves from motor neurons, cranial and dorsal root ganglia was particularly abundant (Fig. 4C, F-H). This observation suggests a tissue-specific translational regulation of Lpp3 in the nervous system.

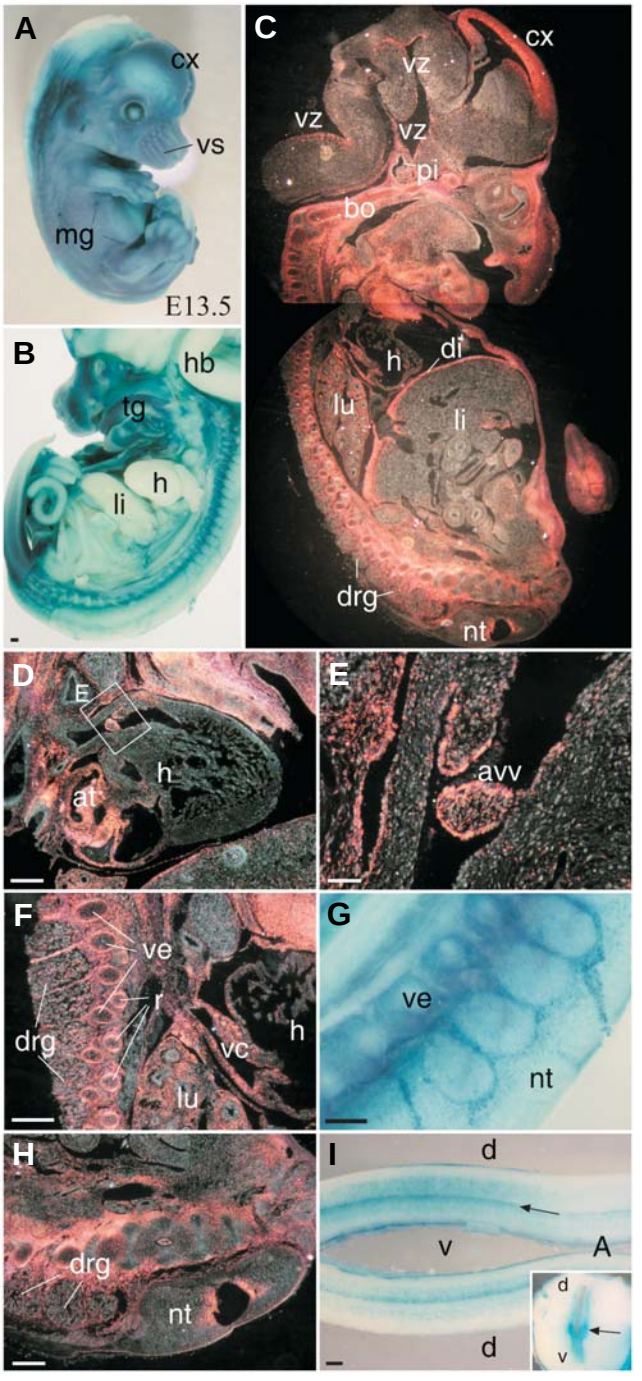

Interestingly *Ppap2b/* Lpp3 expression is abundant in sites where multiple inductive interactions occur such as the limb bud, mammary gland and developing heart valves. In these structures, the convergence of several signaling pathways takes place to give rise to proper development and patterning. In the limb bud, FGF signaling from the AER is fundamental for proper proximal-distal limb patterning and development (Sun *et al.,* 2002, Yu and Ornitz, 2008). Lpp3 is abundantly expressed in the AER between E9.5 - E12.5, fingertips at E13.5 and in the distal mesenchyme around E10.5. It would be interesting to analyze whether expression of *Ppap2b* in the AER is a consequence of Fgf8 signaling. Furthermore, it is temping to speculate that Lpp3 could function as a modulator of Fgf8 signaling in the AER and subjacent mesenchyme in view of its potential impact on Ras activation, through the control of phosphatidic acid and DAG levels. On the other hand, Wnt7a non-canonical signaling from the dorsal ectoderm and Engrailed-1 activity from the ventral ectoderm are both required for D-V limb patterning. While Wnt7a induces Lmx1b expression in the dorsal mesenchyme, β-catenin-induced En1 expression in the ventral ectoderm is required to restrict Lmx1b expression in the ventral mesenchyme (Loomis *et al.,* 1996, Loomis *et al.,* 1998). It is worth noting that Lpp3 is expressed in the distal-dorsal limb mesenchyme at E10.5 partially resembling the Wnt7a-dependent expression of Lmx1b in the limb. It will be interesting to determine whether Lpp3 expression in dorsal domains of the limb is downstream of Wnt7a/Lmx1b and whether it participates in dorsal-ventral and proximal-distal limb patterning.

Ppap2b expression is very abundant in epithelial placodes and mammary buds at E11.5-13.5 embryos. Moreover, it appears progressively in the surrounding mesenchyme after E13.5 while epithelial expression gradually diminishes in E15.5-16.5 (not shown). In the mouse embryo, mammary gland specification is dependent on FGF signals from the ventral-lateral dermomyotome at the level of the milk line and Wnt signals in the milk line ectoderm. Posterior placode formation requires the participation of the same groups of factors but more prominently of Wnt signals (Hens and Wysolmerski, 2005). Contradicting results regarding the participation of epithelial or mesenchymal Wnt signals during mammary bud development exist, using two different TOPGAL reporter transgenics. In one study, β-gal activity was found first in ectodermal cells along the mammary line and latter restricted to epithelial cells of the mam-

Fig. 5. *Ppap2b* expression in E13.5 embryos. *β-galactosidase staining of* Ppap2b^{lacZ} *heterozygous mouse embryos. External* **(A)** *and mid sagittal views* **(B,C)**. **(A-B, G,I)** *Bright field microscopy showing reporter activity in blue.* **(C-F, H)** *Dark field microscopy showing reporter activity in pink or reddish color. Expression in the heart is restricted to the atrium* **(D)** *atrioventricular valves* **(E)** *and superior vena cava* **(F)**. **(F,G)** *Expression in cartilage condensations, lung mesenchyme and dorsal root ganglia. β-gal staining in the neural tube at the sacral* **(H)** *and thoracic* **(I)** *levels.* **(I)** *Open-book preparation of the neural tube. Insert: cross section of the spinal cord showing the position of the cells forming the stripe of cells with expression of β-gal (arrow). A, anterior; at, atrium; avv, developing atrioventricular valve; bo, cartilage primordium of the basioccipital bone; cx, developing cortex; d, dorsal; di, diaphragm; drg, dorsal root ganglion; h, heart; hindbrain li, liver; lu, lung; mg, mammary gland buds; nt, neural tube; pi, pituitary; r, rib cartilage primordium; tg, tongue; v, ventral; vc, vena cava; ve, vertebral cartilage primordium; vs, vibrissae follicles; vz, ventricular zone. Scale bars, 40 μm in (E),; 200 μm in (B,D, F-G).*

mary placodes and buds, with few mesenchymal cells expressing the reporter by E13.5 (Chu *et al.,* 2004). In the other, β-gal expression in the mesenchyme surrounding the mammary placodes started around E11.5 and it was not until E13.5 that it was also found in the bud epithelia, all of these in agreement with nuclear localization of β-catenin (Boras-Granic *et al.,* 2006). The latter work suggests that mesenchymal cells integrate Wnt signals during the early stages of mammary gland development and that epithelial Wnt expression is required later to the progress of mammary gland development. We have previously described that Lpp3 acts as a negative regulator of the canonical Wnt/β-catenin signaling pathway (Escalante-Alcalde *et al.,* 2003). In this sense, *Ppap2b* expression during mammary gland development fits better with the second model where it acts as a negative feedback loop to attenuate canonical Wnt signaling, by restricting Wnt activity in epithelial cells during early mammary gland development and then to restrict Wnt activity in the surrounding mesenchyme.

Ppap2b expression during cardiac valve development was particularly interesting. Abnormalities in heart valves and associated structures are the most common subtype of cardiovascular malformation. Heart valves develop from cardiac cushions produced by endothelial-mesenchymal transition of the endocardial cells with subsequent proliferation and tissue remodeling in specific regions of the heart. Cushions later protrude from the underlying myocardium to form the valve leaflets (Armstrong and Bischoff, 2004, Lincoln *et al.,* 2004). A complex signaling network involving Vegf, Nfat, Notch, Wnt/β-catenin, BMP, TGFβ, ErbB and NF1/Ras has been implicated in the control of heart valve development (Armstrong and Bischoff, 2004). Again, due to the potential effect of Lpp3 in modulating several of these signaling pathways, an essential role for it in heart valve development may be predicted.

During central and peripheral nervous system development, *Ppap2b/* Lpp3 is expressed in a very particular fashion. In the central nervous system, Lpp3 is present predominantly in ventral domains of the neural tube as early as E8.5. In addition it is remarkable that *Ppap2b* is expressed in the notochord. Gene expression and cell type specification in ventral domains of the neural tube are mainly controlled by the secretion of Shh by the notochord and floor plate (Briscoe *et al.,* 2000). In this sense, it is provocative to speculate that Lpp3 expression in the neural tube, notochord and perhaps paraxial mesenchyme (see below) might be regulated by Shh signaling. In support of this idea, an in silico analysis (NCBI DCODE.org Comparative Genomics Developments) of conserved regulatory elements in the *Ppap2b* promoter of rat and mice, revealed the presence of putative binding sites for Gli2, Pax6, Nkx2-2, Nkx6-1 and FoxA2 transcription factors, all participating in the ventral specification of the neural tube (Briscoe *et al.,* 1999, Ding *et al.,* 1998, Ericson *et al.,* 1997, Sander *et al.,* 2000, Sasaki *et al.,* 1997). Assaying whether inhibition of Shh signaling affects the neural expression of Lpp3 and whether the aforementioned putative binding sites are functional will be of significance. Furthermore, it will be interesting to analyze the participation of Lpp3 in the specification of ventral cell types in the neural tube. Up-regulation of *Ppap2b* expression by the treatment with Shh has been recently described in mesenchymal stem cells (Ingram *et al.,* 2008).

As shown, Lpp3 is also abundantly expressed in projecting axons of motor neurons, cranial and dorsal root ganglia neurons. Given that LPA and S1P exhibit a powerful neurite-retraction activity (Postma *et al.,* 1996, Tigyi *et al.,* 1996), it is temping to suggest that Lpp3 expression in these neuronal types might serve to counteract the retractogenic environment caused by such lipids, contributing to the axon outgrowth during mouse development. In support of this idea is the inability of Lpp3 deficient MN differentiated *in vitro* from ES cells to produce neurites (R. Sánchez and D. E-A in preparation).

As previously described, Lpp3 is expressed during embryonic development in several structures where complex signaling networks occur to ensure their proper development and patterning. These observations suggest that Lpp3 expression may play a key role in modulating/integrating multiple signaling pathways during development. This idea rests on the assumption of a precise control of its temporal and spatial expression in conjunction with an accurate regulation of its actions as an intracellular or as a plasma membrane-associated protein. Tissue specific inactivation of *Ppap2b* will help us to address the participation of Lpp3 in the various mentioned developmental processes. Likewise the reporter allele described in this paper will allow us to address some aspects of the transcriptional regulation of Ppap2b during development.

Materials and Methods

Generation of Ppap2^{tm2Stw} *ES cells and mice*

The mouse EST AA276423 IMAGE Consortium clone ID 776179 (Lennon *et al.,* 1996) was used to screen a 129/SvJ mouse genomic BAC library (Research Genetics). From clone BJ4123, a 5.1 XmaI fragment, containing exons 3 and 4, was used to produce an insertion targeting vector with the following configuration: 3 stop codons in 3 frames were introduced upstream of an IRES-lacZ reporter cassette. A PGKneo cassette, flanked by loxP sites, was introduced downstream of the reporter cassette for positive selection. The reporter-positive selection cassette was introduced in the proper orientation into the unique MunI restriction site located in exon 3. This insertion interrupts the protein between C1 and C2 domains essential for the catalytic activity. A TK negative selection cassette was added downstream of the 3' arm and then the vector linearized. W9.5 ES cells were electroporated with the targeting construct selected in the presence of G418 and FIAU and screened for legitimate homologous recombination by Southern (Fig.1). The insertion of the reporter cassette introduces two additional BamHI sites, originating bands of 5.7 or 8.3 kb when using the 5' and 3' probes respectively, in BamHI digested genomic DNA. Out of 117 isolated clones, 24% resulted in the recombined allele. After karyotyping, one clone was selected for derivation of chimeras that were crossed to C57BL6/J females to test germ line transmission and to establish a mouse line designated *Ppap2b^{tm2Stw}*.

Genotyping

For PCR genotyping, a set of three oligonucleotides was designed to distinguish between the wild type and targeted alleles. Primer a is upstream (a. 5' CTG TGC CAT TAG CCA GTC CTT CAC 3') and primer b is downstream (b. 5' TAG TTC TGA ATG TAG CCC TCG GAG 3') of the MunI restriction site fragment in exon 3. In the wild type configuration, these amplify a product of 128 bp. A primer in the floxed PGKneo cassette (c. 5' TTC TAT CGC CTT CTT GAC GAG TTC 3') in combination with primer b amplifies a product of around 700 bp. Alternatively born heterozygous individuals were genotyped using *lacZ* specific primers or β-galactosidase staining of ear fragments.

β-galactosidase staining

Embryos or fragments of tissues were stained as previously described (Hogan *et al.,* 1994). Briefly, tissues were immersed in fixative solution, washed 3 times for 30 min with detergent rinse and then incubated

overnight in staining solution. The samples were embedded in paraffin, sectioned at 6 μm. Sections were visualized and photographed using Nomarski optics (DIC) or dark field illumination in which β-gal staining appeared of pink or reddish color.

Whole mount in situ *hybridization*

Mouse embryos were fixed and processed for *in situ* hybridization as described previously (Hogan *et al.,* 1994). Full length Lpp3 cDNA was cloned into pBluescript(KS) and then linearized with MunI. Anti-sense and sense probes were transcribed using T3 and T7 RNA polymerases respectively.

Whole mount immunohistochemistry

Protein detection was performed as previously described (Hogan *et al.,* 1994). Briefly, embryos were fixed with methanol/DMSO (4:1) and endogenous peroxidase activity was blocked by H_2O_2 treatment. The incubation with the primary antibody (anti-LPP3, 1:200 Upstate) was carried out overnight at 4˚C. Anti-rabbit coupled to peroxidase was used at a dilution of 1:500. After color reaction embryos were post fixed with 4% paraformaldehyde and cleared with BABB for observation and photographic record.

Acknowledgements

We are grateful to T. Rosenbaum and I. Velasco for comments and carefully reading of the manuscript. This work was partially supported by CONACyT 39995 and PAPIIT IN215605.

References

ARMSTRONG, E.J. and BISCHOFF, J. (2004). Heart valve development: endothelial cell signaling and differentiation. *Circ Res* 95: 459-470.

BORAS-GRANIC, K., CHANG, H., GROSSCHEDL, R. and HAMEL, P.A. (2006). Lef1 is required for the transition of Wnt signaling from mesenchymal to epithelial cells in the mouse embryonic mammary gland. *Dev Biol* 295: 219-231.

BRINDLEY, D.N. (2004). Lipid phosphate phosphatases and related proteins: signaling functions in development, cell division, and cancer. *J Cell Biochem* 92: 900-912.

BRINDLEY, D.N., ENGLISH, D., PILQUIL, C., BURI, K. and LING, Z.C. (2002). Lipid phosphate phosphatases regulate signal transduction through glycerolipids and sphingolipids. *Biochim Biophys Acta* 1582: 33-44.

BRINDLEY, D.N. and WAGGONER, D.W. (1998). Mammalian lipid phosphate phosphohydrolases. *J Biol Chem* 273: 24281-24284.

BRISCOE, J., PIERANI, A., JESSELL, T.M. and ERICSON, J. (2000). A homeodomain protein code specifies progenitor cell identity and neuronal fate in the ventral neural tube. *Cell* 101: 435-445.

BRISCOE, J., SUSSEL, L., SERUP, P., HARTIGAN-O'CONNOR, D., JESSELL, T.M., RUBENSTEIN, J.L. and ERICSON, J. (1999). Homeobox gene Nkx2.2 and specification of neuronal identity by graded Sonic hedgehog signalling. *Nature* 398: 622-627.

CHU, E.Y., HENS, J., ANDL, T., KAIRO, A., YAMAGUCHI, T.P., BRISKEN, C., GLICK, A., WYSOLMERSKI, J.J. and MILLAR, S.E. (2004). Canonical WNT signaling promotes mammary placode development and is essential for initiation of mammary gland morphogenesis. *Development* 131: 4819-4829.

DING, Q., MOTOYAMA, J., GASCA, S., MO, R., SASAKI, H., ROSSANT, J. and HUI, C.C. (1998). Diminished Sonic hedgehog signaling and lack of floor plate differentiation in Gli2 mutant mice. *Development* 125: 2533-2543.

ERICSON, J., RASHBASS, P., SCHEDL, A., BRENNER-MORTON, S., KAWAKAMI, A., VAN HEYNINGEN, V., JESSELL, T.M. and BRISCOE, J. (1997). Pax6 controls progenitor cell identity and neuronal fate in response to graded Shh signaling. *Cell* 90: 169-180.

ESCALANTE-ALCALDE, D., HERNANDEZ, L., LE STUNFF, H., MAEDA, R., LEE, H.S., JR GANG, C., SCIORRA, V.A., DAAR, I., SPIEGEL, S., MORRIS, A.J. et al. (2003). The lipid phosphatase LPP3 regulates extra-embryonic vasculogenesis and axis patterning. *Development* 130: 4623-4637.

ESCALANTE-ALCALDE, D., SANCHEZ-SANCHEZ, R. and STEWART, C.L. (2007). Generation of a conditional Ppap2b/Lpp3 null allele. *Genesis* 45: 465-469.

GARCIA-MURILLAS, I., PETTITT, T., MACDONALD, E., OKKENHAUG, H., GEORGIEV, P., TRIVEDI, D., HASSAN, B., WAKELAM, M. and RAGHU, P. (2006). lazaro encodes a lipid phosphate phosphohydrolase that regulates phosphatidylinositol turnover during Drosophila phototransduction. *Neuron* 49: 533-546.

HANYU-NAKAMURA, K., KOBAYASHI, S. and NAKAMURA, A. (2004). Germ cell-autonomous Wunen2 is required for germline development in Drosophila embryos. *Development* 131: 4545-4553.

HENS, J.R. and WYSOLMERSKI, J.J. (2005). Key stages of mammary gland development: molecular mechanisms involved in the formation of the embryonic mammary gland. *Breast Cancer Res* 7: 220-224.

HOGAN, B., BEDDINGTON, R., COSTANTINI, F. and LACY, E. (1994). Manipulating the Mouse Embryo: A Laboratory Manual. Cold Spring Harbor Laboratory Press, Plainview, New York.

HUMTSOE, J.O., FENG, S., THAKKER, G.D., YANG, J., HONG, J. and WARY, K.K. (2003). Regulation of cell-cell interactions by phosphatidic acid phosphatase 2b/VCIP. *EMBO J* 22: 1539-1554.

INGRAM, W.J., MCCUE, K.I., TRAN, T.H., HALLAHAN, A.R. and WAINWRIGHT, B.J. (2008). Sonic Hedgehog regulates Hes1 through a novel mechanism that is independent of canonical Notch pathway signalling. *Oncogene* 27: 1489-1500.

JIA, Y.J., KAI, M., WADA, I., SAKANE, F. and KANOH, H. (2003). Differential localization of lipid phosphate phosphatases 1 and 3 to cell surface subdomains in polarized MDCK cells. *FEBS Lett* 552: 240-246.

KAI, M., SAKANE, F., JIA, Y.J., IMAI, S., YASUDA, S. and KANOH, H. (2006). Lipid phosphate phosphatases 1 and 3 are localized in distinct lipid rafts. *J Biochem* 140: 677-686.

KRAUT, R., MENON, K. and ZINN, K. (2001). A gain-of-function screen for genes controlling motor axon guidance and synaptogenesis in Drosophila. *Curr Biol* 11: 417-430.

LENNON, G.G., AUFFRAY, C., POLYMEROPOULUS, M. and SOARES, M.B. (1996). The I.M.A.G.E. Consortium: an integrated molecular analysis of genomes and their expression. *Genomics* 33: 151-152.

LIGOXYGAKIS, P., STRIGINI, M. and AVEROF, M. (2001). Specification of left-right asymmetry in the embryonic gut of Drosophila. *Development* 128: 1171-1174.

LINCOLN, J., ALFIERI, C.M. and YUTZEY, K.E. (2004). Development of heart valve leaflets and supporting apparatus in chicken and mouse embryos. *Dev Dyn* 230: 239-250.

LONG, J., DARROCH, P., WAN, K.F., KONG, K.C., KTISTAKIS, N., PYNE, N.J. and PYNE, S. (2005). Regulation of cell survival by lipid phosphate phosphatases involves the modulation of intracellular phosphatidic acid and sphingosine 1-phosphate pools. *Biochem J* 391: 25-32.

LOOMIS, C.A., HARRIS, E., MICHAUD, J., WURST, W., HANKS, M. and JOYNER, A.L. (1996). The mouse Engrailed-1 gene and ventral limb patterning. *Nature* 382: 360-363.

LOOMIS, C.A., KIMMEL, R.A., TONG, C.X., MICHAUD, J. and JOYNER, A.L. (1998). Analysis of the genetic pathway leading to formation of ectopic apical ectodermal ridges in mouse Engrailed-1 mutant limbs. *Development* 125: 1137-1148.

MCDERMOTT, M., WAKELAM, M.J. and MORRIS, A.J. (2004). Phospholipase D. *Biochem Cell Biol* 82: 225-253.

MIZUGISHI, K., YAMASHITA, T., OLIVERA, A., MILLER, G.F., SPIEGEL, S. and PROIA, R.L. (2005). Essential role for sphingosine kinases in neural and vascular development. *Mol Cell Biol* 25: 11113-11121.

MOOLENAAR, W.H., VAN MEETEREN, L.A. and GIEPMANS, B.N. (2004). The ins and outs of lysophosphatidic acid signaling. *Bioessays* 26: 870-881.

MOR, A., CAMPI, G., DU, G., ZHENG, Y., FOSTER, D.A., DUSTIN, M.L. and PHILIPS, M.R. (2007). The lymphocyte function-associated antigen-1 receptor costimulates plasma membrane Ras via phospholipase D2. *Nat Cell Biol* 9: 713-719.

POSTMA, F.R., JALINK, K., HENGEVELD, T. and MOOLENAAR, W.H. (1996). Sphingosine-1-phosphate rapidly induces Rho-dependent neurite retraction: action through a specific cell surface receptor. *EMBO J* 15: 2388-2392.

PYNE, S., KONG, K.C. and DARROCH, P.I. (2004). Lysophosphatidic acid and sphingosine 1-phosphate biology: the role of lipid phosphate phosphatases. *Semin Cell Dev Biol* 15: 491-501.

RENAULT, A.D., SIGAL, Y.J., MORRIS, A.J. and LEHMANN, R. (2004). Soma-germ line competition for lipid phosphate uptake regulates germ cell migration and survival. *Science* 305: 1963-1966.

SABA, J.D. (2004). Lysophospholipids in development: Miles apart and edging in. *J Cell Biochem* 92: 967-92.

SANDER, M., PAYDAR, S., ERICSON, J., BRISCOE, J., BERBER, E., GERMAN, M., JESSELL, T.M. and RUBENSTEIN, J.L. (2000). Ventral neural patterning by Nkx homeobox genes: Nkx6.1 controls somatic motor neuron and ventral interneuron fates. *Genes Dev* 14: 2134-2139.

SASAKI, H., HUI, C., NAKAFUKU, M. and KONDOH, H. (1997). A binding site for Gli proteins is essential for HNF-3beta floor plate enhancer activity in transgenics and can respond to Shh in vitro. *Development* 124: 1313-1322.

SCIORRA, V.A. and MORRIS, A.J. (1999). Sequential actions of phospholipase D and phosphatidic acid phosphohydrolase 2b generate diglyceride in mammalian cells. *Mol Biol Cell* 10: 3863-3876.

SIGAL, Y.J., MCDERMOTT, M.I. and MORRIS, A.J. (2005). Integral membrane lipid phosphatases/phosphotransferases: common structure and diverse functions. *Biochem J* 387: 281-293.

STARZ-GAIANO, M., CHO, N.K., FORBES, A. and LEHMANN, R. (2001). Spatially restricted activity of a Drosophila lipid phosphatase guides migrating germ cells. *Development* 128: 983-991.

SUN, W.S., IMAI, A., SUGIYAMA, M., FURUI, T., TAMAYA, T., SAIO, M. and MORRIS, A.J. (2004). Translocation of lysophosphatidic acid phosphatase in response to gonadotropin-releasing hormone to the plasma membrane in ovarian cancer cell. *Am J Obstet Gynecol* 191: 143-149.

SUN, X., MARIANI, F.V. and MARTIN, G.R. (2002). Functions of FGF signalling from the apical ectodermal ridge in limb development. *Nature* 418: 501-508.

TANAKA, M., OKUDAIRA, S., KISHI, Y., OHKAWA, R., ISEKI, S., OTA, M., NOJI, S., YATOMI, Y., AOKI, J. and ARAI, H. (2006). Autotaxin stabilizes blood vessels and is required for embryonic vasculature by producing lysophosphatidic acid. *J Biol Chem* 281: 25822-25830.

TIGYI, G., FISCHER, D.J., SEBOK, A., YANG, C., DYER, D.L. and MILEDI, R. (1996). Lysophosphatidic acid-induced neurite retraction in PC12 cells: control by phosphoinositide-Ca2+ signaling and Rho. *J Neurochem* 66: 537-548.

VAN MEETEREN, L.A., RUURS, P., STORTELERS, C., BOUWMAN, P., VAN ROOIJEN, M.A., PRADERE, J.P., PETTIT, T.R., WAKELAM, M.J., SAULNIER-BLACHE, J.S., MUMMERY, C.L. et al. (2006). Autotaxin, a secreted lysophospholipase D, is essential for blood vessel formation during development. *Mol Cell Biol* 26: 5015-5022.

YU, K. and ORNITZ, D.M. (2008). FGF signaling regulates mesenchymal differentiation and skeletal patterning along the limb bud proximodistal axis. *Development* 135: 483-491.

ZHANG, N., SUNDBERG, J.P. and GRIDLEY, T. (2000). Mice mutant for Ppap2c, a homolog of the germ cell migration regulator wunen, are viable and fertile. *Genesis* 27: 137-140.

ZHANG, N., ZHANG, J., PURCELL, K.J., CHENG, Y. and HOWARD, K. (1997). The Drosophila protein Wunen repels migrating germ cells. *Nature* 385: 64-67.

ZHAO, C., DU, G., SKOWRONEK, K., FROHMAN, M.A. and BAR-SAGI, D. (2007). Phospholipase D2-generated phosphatidic acid couples EGFR stimulation to Ras activation by Sos. *Nat Cell Biol* 9: 706-712.

ZHAO, Y., USATYUK, P.V., CUMMINGS, R., SAATIAN, B., HE, D., WATKINS, T., MORRIS, A., SPANNHAKE, E.W., BRINDLEY, D.N. and NATARAJAN, V. (2005). Lipid phosphate phosphatase-1 regulates lysophosphatidic acid-induced calcium release, NF-kappaB activation and interleukin-8 secretion in human bronchial epithelial cells. *Biochem J* 385: 493-502.

Further Related Reading, published previously in the *Int. J. Dev. Biol.*

See our Special Issue ***Plant Development*** edited by José Luis Micol and Miguel Angel Blázquez at:
http://www.ijdb.ehu.es/web/contents.php?vol=49&issue=5-6

See our recent Special Issue ***Fertilization***, in honor of David L. Garbers and edited by Paul M. Wassarman and Victor D. Vacquier at:
http://www.ijdb.ehu.es/web/contents.php?vol=52&issue=5-6

Apo-14 is required for digestive system organogenesis during fish embryogenesis and larval development
Jian-Hong Xia, Jing-Xia Liu, Li Zhou, Zhi Li and Jian-Fang Gui
Int. J. Dev. Biol. (2008) 52: 1089-1098

Allorecognition mechanisms during ascidian fertilization
Yoshito Harada and Hitoshi Sawada
Int. J. Dev. Biol. (2008) 52: 637-645

Sperm head membrane reorganisation during capacitation
Bart M. Gadella, Pei-Shiue Tsai, Arjen Boerke and Ian A. Brewis
Int. J. Dev. Biol. (2008) 52: 473-480

Mammalian sperm metabolism: oxygen and sugar, friend and foe
Bayard T. Storey
Int. J. Dev. Biol. (2008) 52: 427-437

Enhanced development of porcine embryos cloned from bone marrow mesenchymal stem cells
Hai-Feng Jin, B. Mohana Kumar, Jung-Gon Kim, Hye-Jin Song, Yeon-Ji Jeong, Seong-Keun Cho, Sivasankaran Balasubramanian, Sang-Yong Choe and Gyu-Jin Rho
Int. J. Dev. Biol. (2007) 51: 85-90

Blastula wall invagination examined on the basis of shape behavior of vesicular objects with laminar envelopes
Bojan Bozic, Jure Derganc and Sasa Svetina
Int. J. Dev. Biol. (2006) 50: 143-150

A hypothesis linking low folate intake to neural tube defects due to failure of post-translation methylations of the cytoskeleton
Natalie K. Björklund and Richard Gordon
Int. J. Dev. Biol. (2006) 50: 135-141

Efficient Cre-mediated deletion in cardiac progenitor cells conferred by a 3'UTR-ires-Cre allele of the homeobox gene Nkx2-5.
Edouard G Stanley, Christine Biben, Andrew Elefanty, Louise Barnett, Frank Koentgen, Lorraine Robb and Richard P Harvey
Int. J. Dev. Biol. (2002) 46: 431-439

2006 ISI **Impact Factor = 3.577**